

ERROR PROPAGATION IN BLOCK ADJUSTMENT OF HIGH-RESOLUTION SATELLITE IMAGES

Jacek Grodecki, Manager, Photogrammetric System Engineering
Gene Dial, Director of Product Engineering
James Lutes, Geodetic System Specialist
Space Imaging
12076 Grant Street, Thornton, CO 80241
jgrodecki@spaceimaging.com
jlutes@spaceimaging.com
gdial@spaceimaging.com

ABSTRACT

Due to its superior geometric accuracy characteristics, IKONOS satellite imagery is particularly well suited for large scale mapping applications. Geometric accuracy can be further improved by block adjusting satellite images, with or without ground control. Block adjustment of high-resolution pushbroom satellite images, such as IKONOS, differs significantly from classical aerial triangulation. Error propagation in block adjustment of such images, and hence the final mapping accuracy, depends on multiple factors such as image collection geometry, image collection mode (mono or stereo), and accuracy and distribution of ground control. The paper analyzes in detail the influence of these factors and presents a simplified method for accuracy pre-analysis of block adjustment of high-resolution satellite images. The proposed accuracy pre-analysis methodology is demonstrated using IKONOS image blocks collected in mono and stereo mode.

INTRODUCTION

Superb geometric accuracy of IKONOS imagery makes it particularly well suited for large scale mapping applications. As demonstrated in [Dial and Grodecki, 2002b], geometric accuracy of an uncontrolled IKONOS image is 4 meters RMS per axis, and can be improved even more by block adjusting multiple images, with or without ground control.

High-resolution pushbroom satellite cameras, including IKONOS, use linear sensor arrays that acquire a single image line at an instant of time, each with its own positional and attitude data. Moreover, high-resolution pushbroom cameras have a very narrow field of view, resulting in near linear dependencies between many physical camera model parameters [Grodecki and Dial, 2003]. These and other factors discussed in this paper make the error propagation in high-resolution satellite image blocks significantly different from classical aerial triangulation.

The paper analyzes the impact of such factors as image collection geometry, image collection mode (mono or stereo), and accuracy and distribution of ground control on the geometric accuracy of high-resolution satellite image blocks. For this purpose a simplified block adjustment model is developed using a camera model based on image collection geometry. In addition a geometric interpretation of the error propagation characteristics is given and later shown to agree with experimental results.

IMAGE COLLECTION GEOMETRY

An approximate image collection geometry is described by the sensor azimuth and the sensor elevation angles, as shown in Figure 1. The projection of the line of sight from the target to the satellite onto the horizontal plane at the target location defines the sensor azimuth. The sensor azimuth is measured clockwise from the North. The sensor elevation angle is the angle from the horizon up to the satellite.

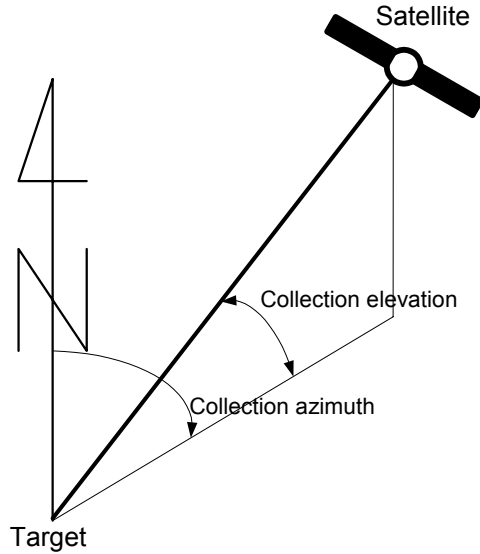


Figure 1. Image collection geometry

Alternatively, image collection geometry can be depicted in a polar coordinate system (see Figure 2). The sensor azimuth is given by the polar angle measured clockwise from the north axis. The sensor elevation angle is specified by the radial coordinate, reaching maximum of 90° at the center of the polar coordinate system and decreasing with the distance from the origin of the polar plot.

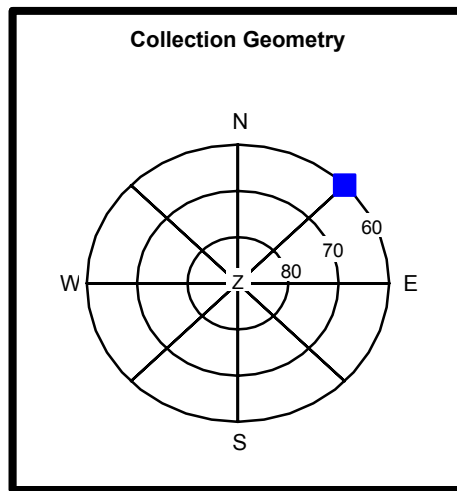


Figure 2. Image collection geometry in a polar coordinate system (azimuth = 45° , elevation = 60°)

The sensor azimuth and the sensor elevation angles are not necessarily constant for a given image strip. Their rate of change depends on the difference between the scan and the orbital velocity vectors. For IKONOS the scan velocity is almost the same as the orbital velocity. As a result, in the “reverse scan” mode, when the scan and the orbital velocity vectors are pointing roughly in the same direction, the sensor azimuth and the sensor elevation angles can be assumed to be constant for the entire IKONOS image strip. In contrast, in the “forward scan” mode the scan and the orbital velocity vectors are pointing in the opposite directions resulting in approximately 1 degree/second rate of change of the sensor elevation angle.

For IKONOS, the image collection geometry data including the sensor azimuth angle, the sensor elevation angle, and the scan mode are provided as part of the image metadata.

BLOCK ADJUSTMENT

A method for block adjusting high-resolution pushbroom imagery described by RPC camera model is given in [Grodecki and Dial, 2003]. It can be shown [Dial and Grodecki, 2002a] and [Grodecki and Dial, 2003] that two offset parameters plus, optionally for longer strips, two drift parameters can completely and accurately characterize IKONOS sensor errors. A line offset parameter models effects of orbit, attitude, and residual interior orientation errors in the line direction. As discussed in [Dial and Grodecki, 2002a] and [Grodecki and Dial, 2003], for narrow field of view instruments with accurate *a priori* orientation data, all of these physical parameters have the same net effect of displacing images in line. Likewise, the sample offset parameter models the same errors in the sample direction. A parameter proportional to the line coordinate can be added to model gyro drift errors. For IKONOS, these errors have been found to be less than a few pixels per 100km [Grodecki and Dial, 2003] and thus negligible for all but very long strips.

A similar method of exterior orientation bias compensation for IKONOS imagery described by RPCs has been independently proposed by [Fraser et al., 2002], and [Fraser and Hanley, 2003].

Grodecki and Dial [2002], Grodecki and Dial [2003], and Fraser and Hanley [2003] have demonstrated effectiveness and robustness of this simple RPC-based block adjustment model. Grodecki and Dial [2002] used both an offset-only 2-parameter model and a full 4-parameter model to block adjust a large IKONOS stereo block. The adjustment results showed only a marginal improvement with a full 4-parameter model, demonstrating that an offset-only model is sufficiently accurate for strip lengths of up to 50 km. [Fraser and Hanley, 2003] used an offset-only camera model with RPCs and a large number of independent check points to quantify post-adjustment geometric accuracy of IKONOS imagery, showing that it is possible to achieve sub-meter accuracy with as few as 1 to 2 ground control points.

AZ-EL CAMERA MODEL

Assuming constant image collection geometry one can express the object-image relationship in terms of the sensor azimuth and the sensor elevation angles. As discussed before, IKONOS sensor model errors can be accurately characterized by two offset parameters. Combining such two offset parameters with the image collection geometry results in the Az-El block adjustment model given below. In a map coordinate system (X, Y), with the line and sample image coordinates resampled to the map coordinate system at 1m GSD, the Az-El block adjustment model is expressed as:

$$\begin{aligned} X_{i_{image}} &= CS0 + X_{i_{object}} + Z_{i_{object}} \cot El \sin Az \\ Y_{i_{image}} &= CL0 + Y_{i_{object}} + Z_{i_{object}} \cot El \cos Az \end{aligned}$$

where:

$X_{i_{image}}, Y_{i_{image}}$ are the image positions of a GCP or a tie point, expressed in the map coordinate system (X,Y)

$X_{i_{object}}, Y_{i_{object}}, Z_{i_{object}}$ are the object space coordinates of a GCP or a tie point, and

El, Az are the sensor elevation and azimuth angles.

$CS0, CL0$ are the image offset parameters.

GEOMETRIC INTERPRETATION

Due to the coplanarity requirement, the object space rays defined by a pair of conjugate image points on two overlapping images and the line connecting the perspective center positions for each image point define a plane. In the Az-El model, all such planes for a given image pair are parallel. Because of the coplanarity condition, error reduction occurs in the direction perpendicular to the plane defined by the target and both satellite positions. As seen

in Figure 3 below, this direction is defined by the projection of the cross product between the unit line-of-sight (LOS) vectors to each satellite position onto the XY mapping plane.

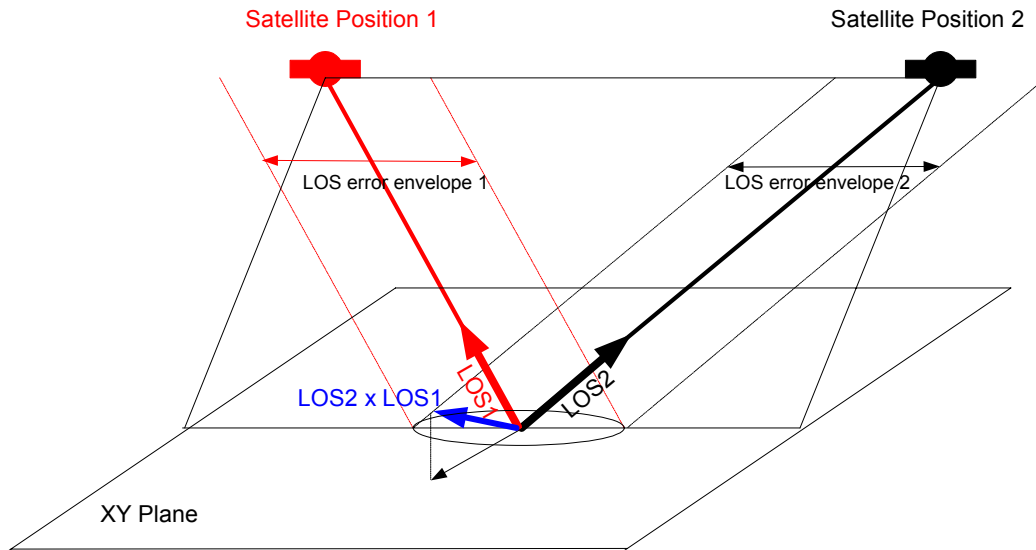


Figure 3. Coplanarity condition

Additional insight can be gained by analyzing the error propagation geometry in the plane defined by the unit LOS vectors to each satellite position, originating from the target position. As seen in Figure 4 below, the uncertainty of a line of sight in one image, due to errors in attitude and ephemeris, is not affected by the amount of uncertainty associated with a line of sight of an adjacent image. Even if one of the images had no error, the LOS of the second image could still move freely as indicated by the blue line in Figure 4, and thus the error envelope of the LOS in the second image would remain exactly the same. Thus, fixing one image by a GCP has no effect on the accuracy of the second image – along the direction defined by the aforementioned plane.

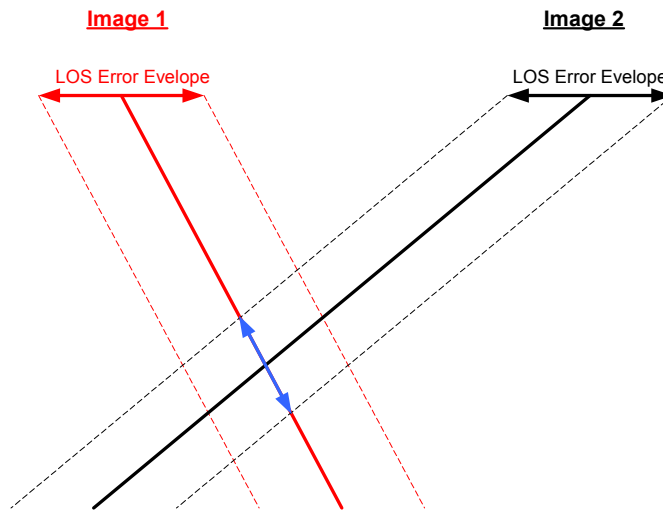


Figure 4. Error Propagation Geometry

ERROR PROPAGATION EXAMPLES

The Az-El block adjustment model was used to generate all error propagation examples presented in this section. An interactive ArcGIS based utility was developed to facilitate analysis and display of the error propagation results. It allows the user to specify the image location and the collection geometry, the placement of tie points and GCPs, and *a priori* sigmas for the image offset parameters and the GCP and tie point object coordinates.

Error Propagation in Mono Blocks

Assumptions. Following the results of an accuracy study given in [Dial and Grodecki, 2002b], it is assumed that all images have *a priori* sigmas of 4 meters in line and sample. Image coordinates of tie points and GCPs are assumed to be measured to 0.3 pixel accuracy at 1-sigma. All images have a nominal footprint size of 11km by 11km. The images are collected either from the north (first and third image) or from the south (second and fourth image), as shown in Figure 5.

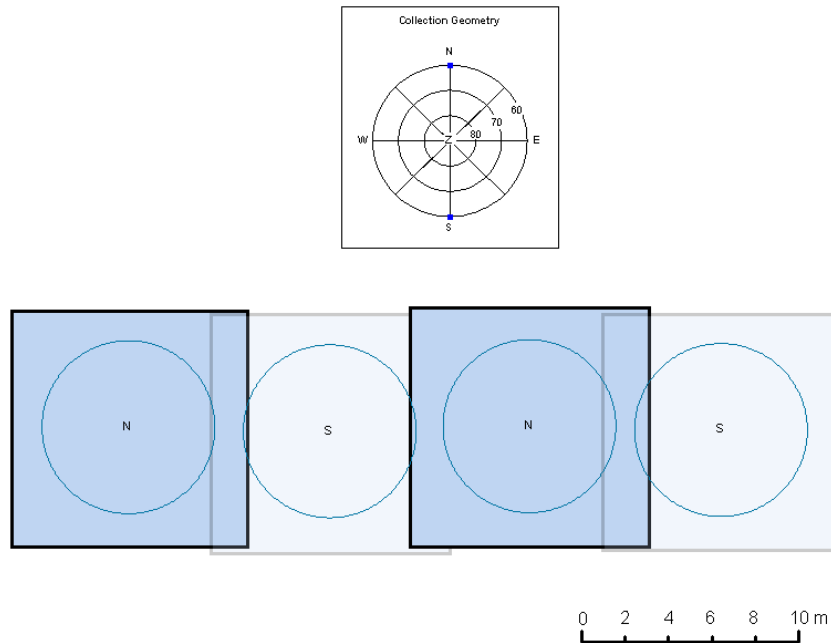


Figure 5. North-South collection geometry. The *a priori* error ellipses are shown in blue.

Tie-pointing and block adjusting the north-south mono block shown above, with no ground control, results in reduction of a posteriori errors in the east-west direction only, as shown in Figure 6 below.

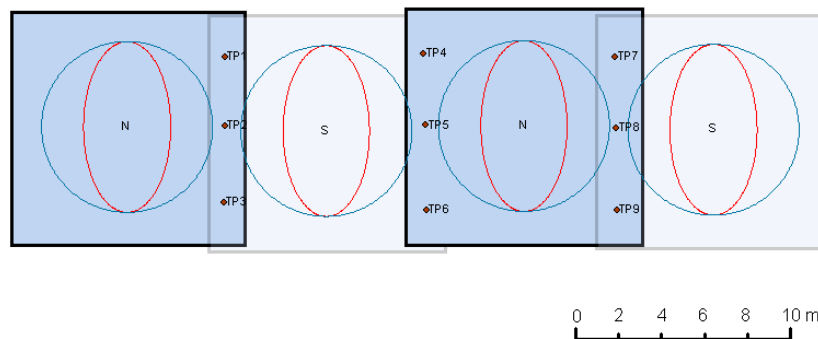


Figure 6. Block adjustment with no GCPs. The *a posteriori* error ellipses are shown in red. The *a priori* error ellipses are shown in blue.

Block adjustment of the same block with a single monoscopic GCP in the first image results in a 2-dimensional error reduction in the first image. The GCP reduces errors in the east-west direction in subsequent images but, as seen in Figure 7 below, there is no further error reduction in the north-south direction beyond the first image.

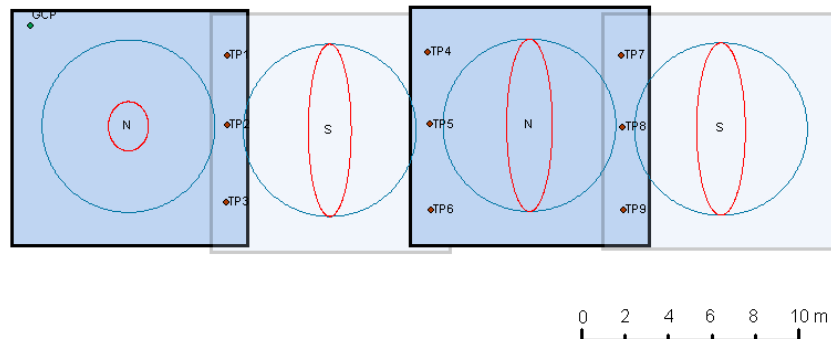


Figure 7. Block adjustment with one monoscopic GCP. The *a posteriori* error ellipses are shown in red. The *a priori* error ellipses are shown in blue.

Block adjustment with a single GCP in the overlap area between the first and the second image results in a 2-dimensional error reduction in both images. The errors in the east-west direction are reduced in subsequent images but, as seen in Figure 8 below, there is no error reduction in the north-south direction beyond the first two images.

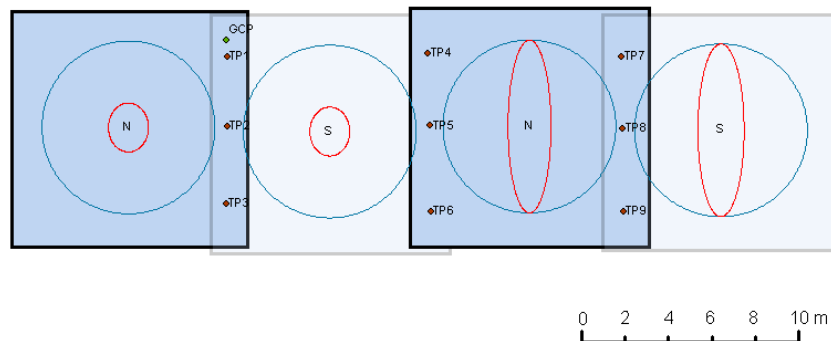


Figure 8. Block adjustment with one stereoscopic GCP. The *a posteriori* error ellipses are shown in red. The *a priori* error ellipses are shown in blue.

Block adjustment with two monoscopic GCPs, one in each corner of the block, results in a 2-dimensional error reduction in the corner images. As before, the errors are reduced in the east-west direction but, as seen in Figure 9 below, there is no error reduction in the north-south direction in the remaining two images.

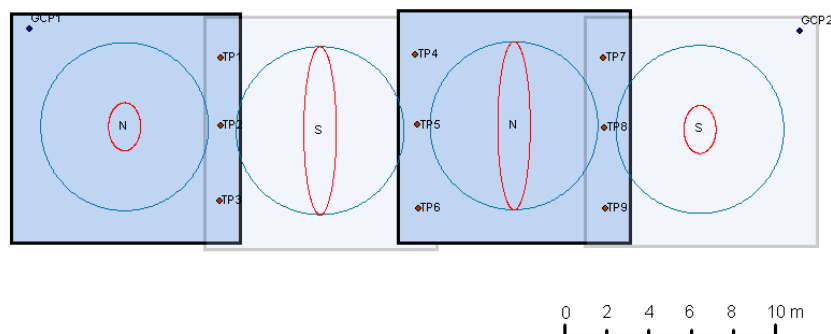


Figure 9. Block adjustment with two monoscopic GCPs. The *a posteriori* error ellipses are shown in red. The *a priori* error ellipses are shown in blue.

Only block adjustment with a GCP in each image (or equivalently with two stereoscopic GCPs) reduces 2-dimensional errors in all images, as seen Figure 10 below. It is seen, that due to the influence of collection geometry, even with a GCP in each image, the *a posteriori* error ellipses retain the north-south orientation.

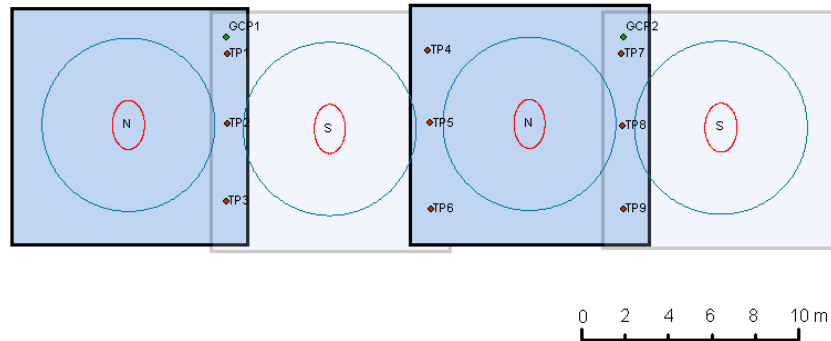


Figure 10. Block adjustment with two stereoscopic GCPs. The *a posteriori* error ellipses are shown in red. The *a priori* error ellipses are shown in blue.

As seen in Figure 11 and Figure 12 below, introduction of vertical constraints reduces errors in the north-south direction. Figure 11 shows the results with 10m (1-sigma) vertical constraints, which would be roughly equivalent to constraining tie points to a USGS DEM. It is seen that the error reduction in the north-south direction is minimal.

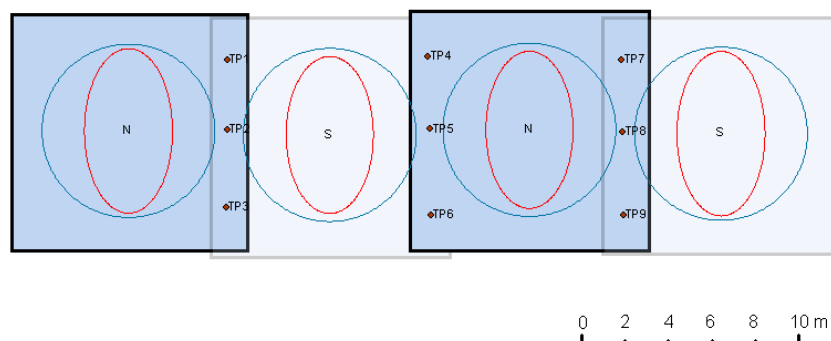


Figure 11. Block adjustment with vertical constraints (10m at 1-sigma). The *a posteriori* error ellipses are shown in red. The *a priori* error ellipses are shown in blue.

Figure 12 shows the results with 1m (1-sigma) vertical constraints, which would be roughly equivalent to constraining tie points to a LIDAR DEM. It is seen that the error reduction in the north-south direction is considerable, resulting in nearly circular *a posteriori* error ellipses.

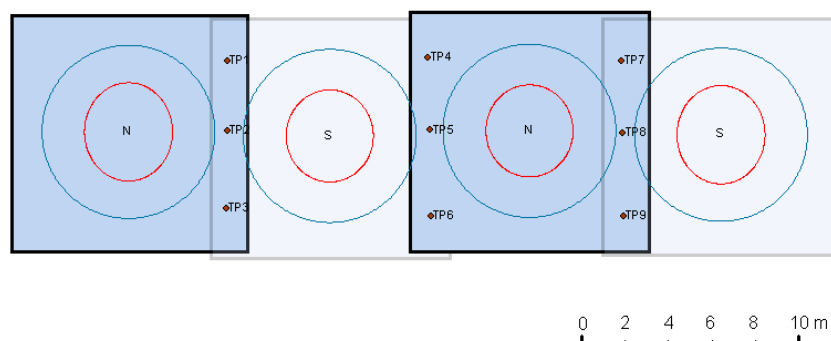


Figure 12. Block adjustment with vertical constraints (1m at 1-sigma). The *a posteriori* error ellipses are shown in red. The *a priori* error ellipses are shown in blue.

Error Propagation in Stereo Blocks

Assumptions. All images have *a priori* sigmas of 4 meters in line and sample. Image coordinates of tie points and GCPs are measured to 0.3 pixel accuracy at 1-sigma. All images have a nominal footprint size of 11 km by 11 km. In each stereo pair, one image is collected from the north while the other is collected from the south, each at 70 deg elevation angle, as shown in Figure 13.

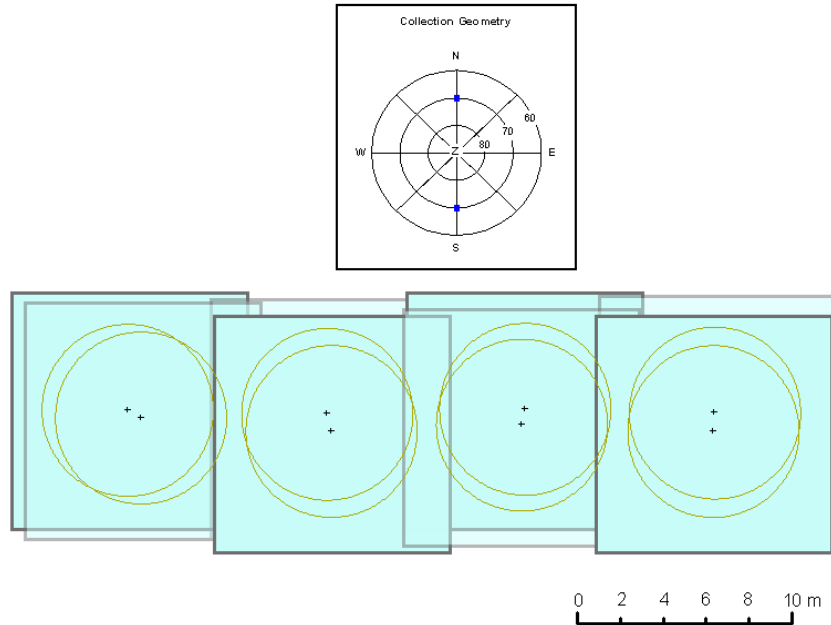


Figure 13. Stereo block. The *a priori* error ellipses are shown in yellow.

As shown in Figure 14 below, as opposed to mono blocks, tie-pointing and block adjusting with no GCPs results in 2-dimensional reduction of *a posteriori* errors in all images.

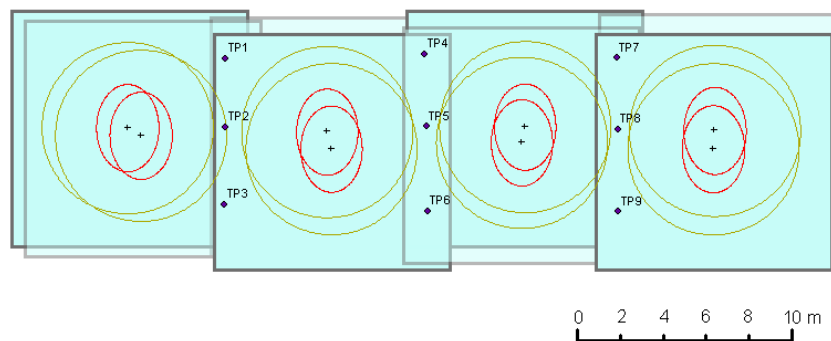


Figure 14. Block adjustment with no GCPs. The *a posteriori* error ellipses are shown in red. The *a priori* error ellipses are shown in yellow.

Block adjustment with a single GCP in the first image pair results in a 2-dimensional error reduction for all images in the block, essentially fixing the entire block.

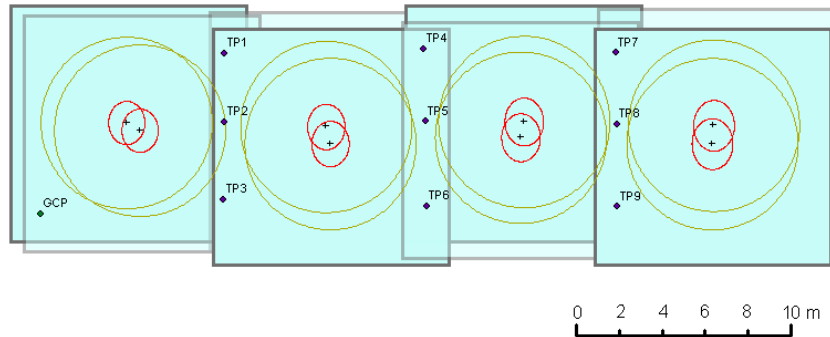


Figure 15. Block adjustment with one GCP. The *a posteriori* error ellipses are shown in red. The *a priori* error ellipses are shown in yellow.

Block adjustment with two GCPs further reduces errors, as seen in Figure 16 below.

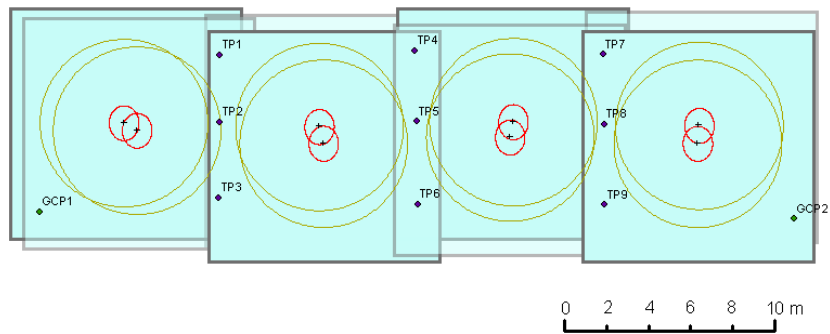


Figure 16. Block adjustment with two GCPs. The *a posteriori* error ellipses are shown in red. The *a priori* error ellipses are shown in yellow.

Constraining tie points vertically to 10m at 1-sigma results in no reduction of *a posteriori* errors.

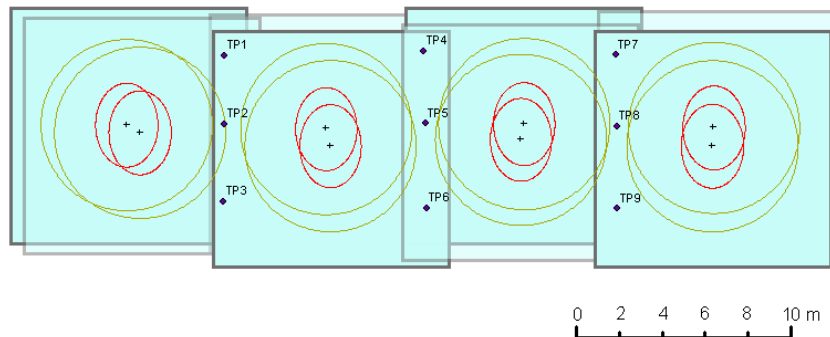


Figure 17. Block adjustment with vertical constraints (10m at 1-sigma). The *a posteriori* error ellipses are shown in red. The *a priori* error ellipses are shown in blue.

Contrary to what we have seen in the mono blocks, constraining tie points vertically to 1m at 1-sigma improves only slightly the *a posteriori* errors.

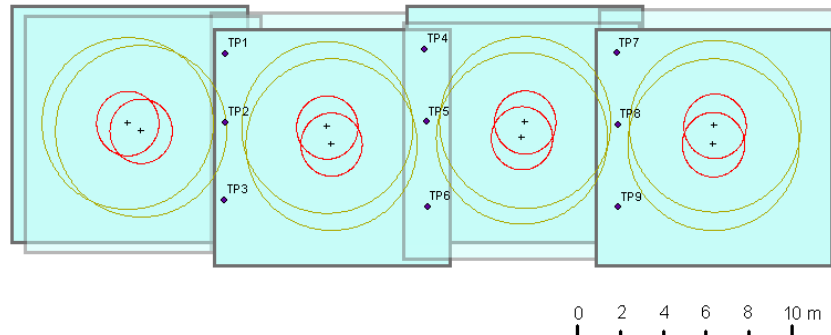


Figure 18. Block adjustment with vertical constraints (1m at 1-sigma). The *a posteriori* error ellipses are shown in red. The *a priori* error ellipses are shown in blue.

CONCLUSIONS

It has been shown that the error propagation in high-resolution satellite image blocks depends strongly on image collection geometry. For mono blocks the error improvement occurs only in one direction.

Error propagation in mono blocks is less favorable than error propagation in stereo blocks. In particular GCPs do not propagate 2-dimensionally across the block of monoscopic images. Stereo blocks are different. A single GCP can control the entire stereo block.

Adding vertical constraints can improve error propagation in mono blocks. However, weak vertical constraints do not result in a significant improvement.

Adding vertical constraints to stereo blocks results in no appreciable improvement of *a posteriori* errors.

REFERENCES

- Dial, Gene and Jacek Grodecki (2002a). "Block Adjustment with Rational Polynomial Camera Models." *Proceedings of ASPRS 2002 Conference*, Washington, DC, April 22-26, 2002.
- Dial, Gene and Jacek Grodecki (2002b). "IKONOS Accuracy without Ground Control." *Proceedings of ISPRS Commission I Mid-Term Symposium*, Denver, CO, November 10-15, 2002.
- Fraser, Clive S., Hanley, Harry B. and T. Yamakawa (2002). "High-Precision Geopositioning from IKONOS Satellite Imagery." *Proceedings of ASPRS 2002 Conference*, Washington, DC, April 22-26, 2002.
- Fraser, Clive S. and Harry B. Hanley (2003). "Bias Compensation in Rational Functions for Ikonos Satellite Imagery." *Photogrammetric Engineering & Remote Sensing*, 69(1): 53-57.
- Grodecki, Jacek (2001). "IKONOS Stereo Feature Extraction—RPC Approach." *Proceedings of ASPRS 2001 Conference*, St. Louis, April 23-27, 2001.
- Grodecki, Jacek and Gene Dial (2001). "IKONOS Geometric Accuracy." *Proceedings of Joint Workshop of ISPRS Working Groups I/2, I/5 and IV/7 on High Resolution Mapping from Space 2001*, University of Hannover, Hannover, Germany, Sept 19-21, 2001.
- Grodecki, Jacek and Gene Dial (2002). "IKONOS Geometric Accuracy Validation." *Proceedings of ISPRS Commission I Mid-Term Symposium*, Denver, CO, November 10-15, 2002.
- Grodecki, Jacek and Gene Dial (2003). "Block Adjustment of High-Resolution Satellite Images Described by Rational Polynomials." *Photogrammetric Engineering & Remote Sensing*, 69(1): 59-68.
- Tao, C. Vincent and Yong Hu (2001). "A Comprehensive Study of the Rational Function Model for Photogrammetric Processing." *Photogrammetric Engineering & Remote Sensing*, 67(12): 1347-1357.